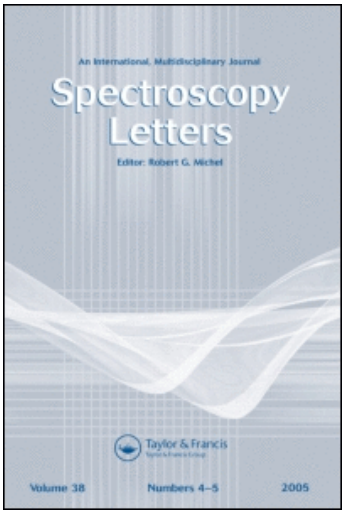

Spectroscopy Letters
Publication details, including instructions for authors and subscription information:
http://www.informaworld.com/smpp/title~content=t713597299

Microscopic Analysis of 5*d* States Splitting and Charge Transfer Energies Dependence on Interionic Distance in Alkaline Earth Fluorides Doped with Light Trivalent Lanthanides

Mikhail G. Brik[a]; Kazuyoshi Ogasawara[a]
[a] Department of Chemistry and Open Research Center for Coordination Molecule-based Devices, School of Science and Technology, Kwansei Gakuin University, Hyogo, Japan

To cite this Article Brik, Mikhail G. and Ogasawara, Kazuyoshi(2007) 'Microscopic Analysis of 5*d* States Splitting and Charge Transfer Energies Dependence on Interionic Distance in Alkaline Earth Fluorides Doped with Light Trivalent Lanthanides', Spectroscopy Letters, 40: 2, 221 — 235
To link to this Article: DOI: 10.1080/00387010701247290
URL: http://dx.doi.org/10.1080/00387010701247290

Spectroscopy Letters, 40: 221–235, 2007

ISSN 0038-7010 print/1532-2289 online
DOI: 10.1080/00387010701247290

Microscopic Analysis of 5*d* States Splitting and Charge Transfer Energies Dependence on Interionic Distance in Alkaline Earth Fluorides Doped with Light Trivalent Lanthanides

Mikhail G. Brik and Kazuyoshi Ogasawara
Department of Chemistry and Open Research Center for Coordination Molecule-based Devices, School of Science and Technology, Kwansei Gakuin University, Hyogo, Japan

Abstract: A first principles fully relativistic analysis (K. Ogasawara et al., *Phys. Rev. B* **2001**, 64, 115413) of the dependence of 5*d* orbitals splitting (10*Dq*) and charge transfer (CT) energies on interionic distance has been performed for light lanthanides (Ce^{3+}, Pr^{3+}, Nd^{3+}) in CaF_2, SrF_2, BaF_2 crystals. The salient feature of the method is that four-component molecular orbitals (MO) composed of atomic wave functions are used as the basis set. Without any fitting parameter, the power dependencies for 10*Dq* and linear dependencies for the CT energies on the distance between rare-earth (RE) ions and ligands were obtained. A comparison with experimental values is discussed.

Keywords: Charge transfer transitions, crystal field, first principles calculations, trivalent rare earth ions

Received 31 May 2006, Accepted 11 July 2006
The authors were invited to contribute this paper to a special issue of the journal entitled "Spectroscopy of Lanthanide Materials." This special issue was organized by Professor Peter Tanner, City University of Hong Kong, Kowloon.
Address correspondence to Mikhail G. Brik, Fukui Institute for Fundamental Chemistry, Kyoto University, 34-4, Takano-Nishihiraki-cho, Sakyo-ku, Kyoto 606-8103, Japan. E-mail: brik@fukui.kyoto-u.ac.jp

INTRODUCTION

Intensive studies of the intraconfigurational $4f \rightarrow 4f$ transitions of trivalent lanthanides in the past several decades resulted in the development of several theoretical models for the description of their main spectroscopic features.[1,2] However, detailed and consistent studies of the high-lying $4f$ and $5d$ energy levels of trivalent rare-earth ions (RE^{3+}) became possible only quite recently because of experimental limitations. Now this field is extensively studied because of the rapidly growing demand for luminescent materials and solid-state lasers in the ultraviolet or vacuum ultraviolet spectral regions. Lanthanide absorption spectra in the ultraviolet (UV) and vacuum ultraviolet (VUV) spectral regions are complicated due to overlap of the high-lying $4f \rightarrow 4f$ transitions, interconfigurational $4f \rightarrow 5d$ and $4f \rightarrow 6s$ transitions together with possible charge transfer (CT) bands, which makes the spectra difficult to analyze. Recently, experimental and theoretical works (Refs. 3–16, and references therein) allowed for understanding, successful interpretation, and modeling of many UV and VUV spectra of trivalent lanthanides.

In the current work, we report on the results of the detailed first-principles microscopic studies of the $5d$ orbitals splitting and CT transitions for light trivalent lanthanides (Ce^{3+}, Pr^{3+}, Nd^{3+}) in CaF_2, SrF_2, and BaF_2 crystals. Without introducing any fitting parameters, we obtain the dependencies of the $10Dq$ parameter for the $5d$ orbitals and energies of several types of CT transitions on distance between RE^{3+} and F^- in all above-mentioned hosts. The obtained results can be used for interpretation of the pressure dependence of the absorption spectra of Ce^{3+}, Pr^{3+}, Nd^{3+} ions in fluoride lattices. To the best of our knowledge, this is the first attempt of this kind. The paper is organized as follows: in the next section we briefly describe the method of calculations. Then we proceed with presentation of the obtained results, analysis of common trends between considered systems, and discussion of the comparison between the calculated and experimental results (when the latter ones are available).

METHOD OF CALCULATIONS

The method employed in the current calculations is the fully relativistic discrete variational multi-electron (DVME) method developed by Ogasawara et al.[17] This is a configuration-interaction (CI) calculation program, which makes use of the four-component fully relativistic molecular spinors obtained by the discrete-variational Dirac–Slater (DV-DS) cluster calculations.[18] The DVME method is based on the numerical solution of the many-electron Dirac equation, and its main advantages are as follows: 1) the first-principles method without any phenomenological parameters (this is especially important for the development of new materials, prediction of their expected

properties, and analysis of the common trends between similar compounds); 2) very wide area of applications: to any atom or ion in any symmetry from spherical to C_1 for any energy interval from the infrared to the X-ray spectral regions; 3) possibility to take into account all effects of chemical bond formation such as covalency, ionicity, and configuration interactions; 4) potential to calculate a wide variety of physical properties (like transition probabilities, for example) using the obtained wave functions of the corresponding energy levels. All relativistic effects, such as spin-orbit interaction and dependence of mass on velocity, are no longer considered as small perturbations but are taken into account from the very first step of calculations. The key idea of the method is that the molecular orbitals (MO) consisting of the wave functions of an impurity ion and ligands are used throughout the calculations rather than atomic wave functions. This makes the effects of the covalent bond formation in a cluster to be taken into account explicitly, because the percentage contribution of wave functions of different ions to any MO can be readily evaluated.

Because detailed description of the method can be found in the literature (the reader is kindly advised to refer to Refs. 15, 17, 19–23), for the sake of brevity we will not go into further detail but mention that recently this method has been successfully applied to the analysis of the $4f$–$5d$ absorption spectra of various trivalent lanthanides in $LiYF_4$,[15] high-lying $4f$ and $5d$ states of free trivalent lanthanides,[19,20] calculations of the X-ray absorption near edge structure (XANES) spectra of transition metal ions,[21] comparative study of the Cr^{3+} absorption spectra in $ZnAl_2S_4$ and $ZnGa_2O_4$ crystals,[22] and study of the covalence effects for $3d^3$ ions in the $SrTiO_3$ crystal.[23]

RESULTS OF CALCULATIONS AND DISCUSSION

All crystals considered in this paper belong to the same space group *Fm-3m* (space group number 225). Divalent cations (Ca^{2+}, Sr^{2+}, Ba^{2+}) substituted for by trivalent RE ions are surrounded by eight fluorine ions (Fig. 1). The lattice constant a equals 5.4712 Å,[24] 5.8000 Å,[25] and 6.1964 Å[26] for CaF_2, SrF_2, and BaF_2, respectively.

Cubic clusters $[REF_8]^{5-}$ (with RE = Ce, Pr, Nd) embedded into the effective Madelung potential created by the point charges placed at the crystal lattice sites were used in the calculations with atomic orbitals from $1s$ to $6p$ for RE^{3+} ions and from $1s$ to $2p$ for F^- ions. In the 8-fold coordination, d states split into e_g and t_{2g} orbitals, with the former being the ground state and the latter situated above it with energy separation of $10Dq$.[27]

It is well-known that dependence of $10Dq$ on the "impurity ion–ligand" chemical bond length R in the vicinity of the equilibrium position can be represented by the following expression:[28]

$$10Dq = \frac{K}{R^n}, \tag{1}$$

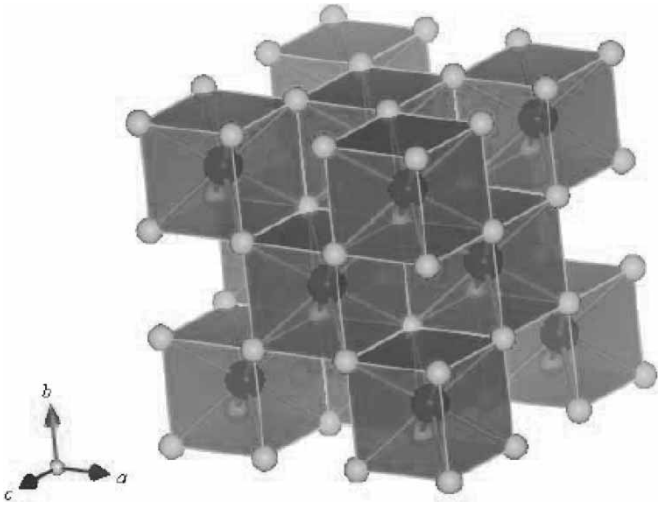

Figure 1. The crystal structure of BaF_2. Barium ions are at the centers of cubes formed by eight fluorine ions. Orientation of the crystallographic axes is shown. Drawn with VENUS developed by Izumi and Dilanian.

where K is a constant, and $n = 5$ in the framework of the point charge model. However, the values of $10Dq$ obtained by using the point charge approximation are significantly lower than experimental results, and the value of n very often is different from 5,[28] thus showing that more elaborated than point charge model approaches should be used for microscopic analysis of the crystal field effects on the electronic states of an impurity ion.

Figure 2 shows the calculated dependencies of the $10Dq$ parameter for $5d$ states (defined as the difference between the barycenters of the groups arising from the t_{2g} and e_g orbitals—the same procedure has been adopted in Refs. 29 and 30 for analysis of experimental spectra) on interionic separation for Ce^{3+}, Pr^{3+}, $Nd^{3+}5d$ states in CaF_2, SrF_2, and BaF_2 crystals. Power approximations of the calculated values (shown by filled symbols) are given in each figure as well along with equations of the fitting lines. RE^{3+}–F^- distances were chosen to vary between $0.92r_0$ and $1.08r_0$ with r_0 being the cation–fluorine separation in the host crystal. As seen from the figures, the value of n differs from 5—the value predicted by the point charge model of crystal field. In each considered crystal, the values of $10Dq$ decrease with increasing RE^{3+} atomic number, as a consequence of the lanthanide contraction. Additionally, the values of crystal field strength for each considered ion decrease in the following direction: $10Dq(CaF_2) > 10Dq(SrF_2) > 10Dq(BaF_2)$, following the increase in the same direction of the crystal lattice constant. For all crystals, the values of n follow the trend: $n(Ce^{3+}) > n(Pr^{3+}) > n(Nd^{3+})$.

Table 1 shows available experimental data on $10Dq$ for the considered systems (though we did not find corresponding experimental data for Nd^{3+},

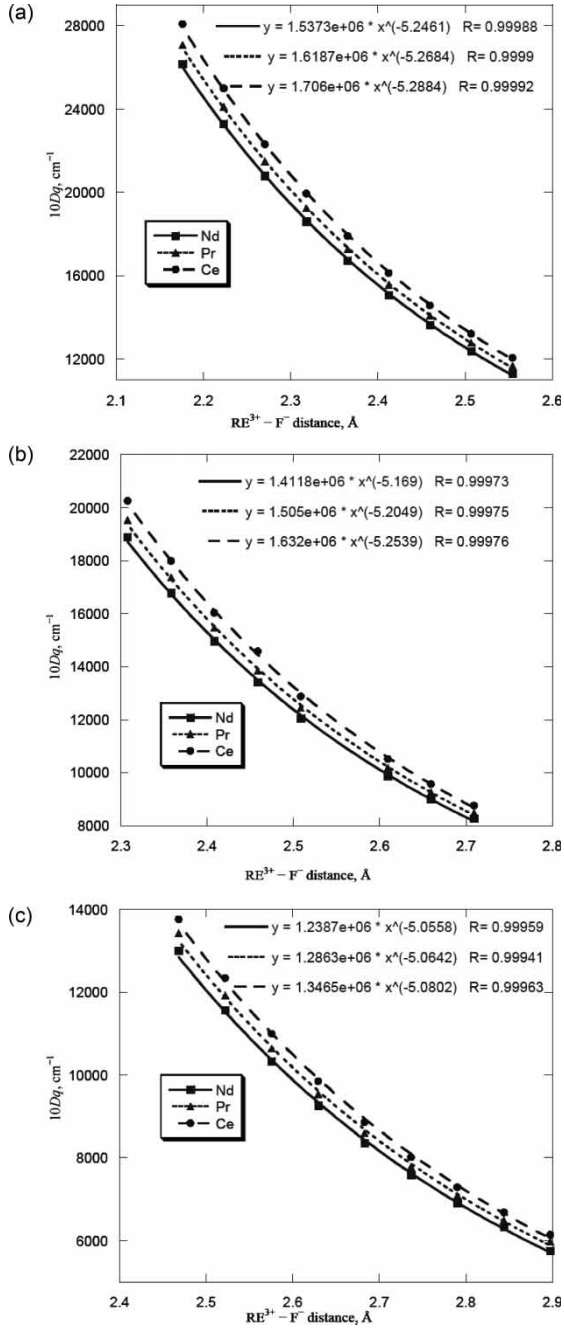

Figure 2. Dependence of 10*Dq* parameter on RE^{3+}–F^{-} distance for 5*d* states of Ce^{3+}, Pr^{3+}, Nd^{3+} in CaF_2, SrF_2, BaF_2 crystals (a, b, and c, respectively). Equations of the approximating lines are also shown.

Table 1. Experimental values of $10Dq$ for Ce^{3+} and Pr^{3+} ions in CaF_2, SrF_2, and BaF_2 crystals and estimated RE–$F^{—}$ distances

RE^{3+}	Experimental value of $10Dq$ ($cm^{—1}$)	Estimated RE^{3+}–$F^{—}$ distance, (Å) (this work)
	CaF_2	
Ce^{3+}	12,200[29]	2.545
Pr^{3+}	12,900[30]	2.502
	SrF_2	
Ce^{3+}	11,200[29]	2.581
Pr^{3+}	11,700[30]	2.542
	BaF_2	
Ce^{3+}	10,800[29]	2.585
Pr^{3+}	10,400[30]	2.589

for the sake of completeness of our study of light lanthanides, we keep the results of calculations for this ion as well). Using these values and obtained power approximations, we estimated the RE^{3+}–F^{-} distances, which are given in Table 1 as well. Because the electrical charges and ionic radii of the substituted and substituting ions are different, actual RE^{3+}–F^{-} distances should be different from the distances between divalent cations and F^{-} in undoped crystals.

Figures 3 to 5 show dependencies of the $2p$ (F^{-}) $\rightarrow$ $4f$ (RE^{3+}) and $2p$ (F^{-}) $\rightarrow$ $6s$ (RE^{3+}) CT transition energies and $4f$ (RE^{3+})–$6s$ (RE^{3+}) transition. All these dependencies are linear; this result is similar to that one obtained for the "ligand–metal" CT transitions for $3d$ ions in oxides.[31]

For both CT transitions, their energies decrease in the series $Ce^{3+} > Pr^{3+} > Nd^{3+}$ and $CaF_2 > SrF_2 > BaF_2$. However, the first trend becomes inverted when considering the $4f$(RE^{3+})–$6s$ (RE^{3+}) transition. Such behavior can be understood by analyzing the MO diagram (Fig. 6). Figure 6 shows the highest MO of Ce^{3+}, Pr^{3+}, and Nd^{3+} in CaF_2. As seen from the figure, MO of RE^{3+} is lower when going from Ce^{3+} to Nd^{3+}, but decrease in the energy of the $4f$ orbitals (about 3 eV) is significantly greater than decrease in the energy of $6s$ orbitals (less than 1 eV). As a result, energies of the $4f$ (RE^{3+})–$6s$ (RE^{3+}) are in the following order: $Nd^{3+} > Pr^{3+} > Ce^{3+}$. Table 2 summarizes information presented in Figures 2 to 5.

Calculated energies of various transitions of Ce^{3+} and Pr^{3+} ions (in comparison with experimental data) are shown in Table 3. Energies of the CT and $4f$ (RE^{3+})–$6s$ (RE^{3+}) transitions were estimated using the linear approximations from Figures 2 to 6 and RE^{3+}–F^{-} distances from Table 1; energies of $4f$ (RE^{3+})–$5d$ (RE^{3+}) transitions were estimated from the diagram in Figure 6 for CaF_2 (and similar diagrams for SrF_2 and BaF_2, not shown in the current paper). In principle, there is reasonable agreement between our calculated values and experimental data reported by Loh[29,30]

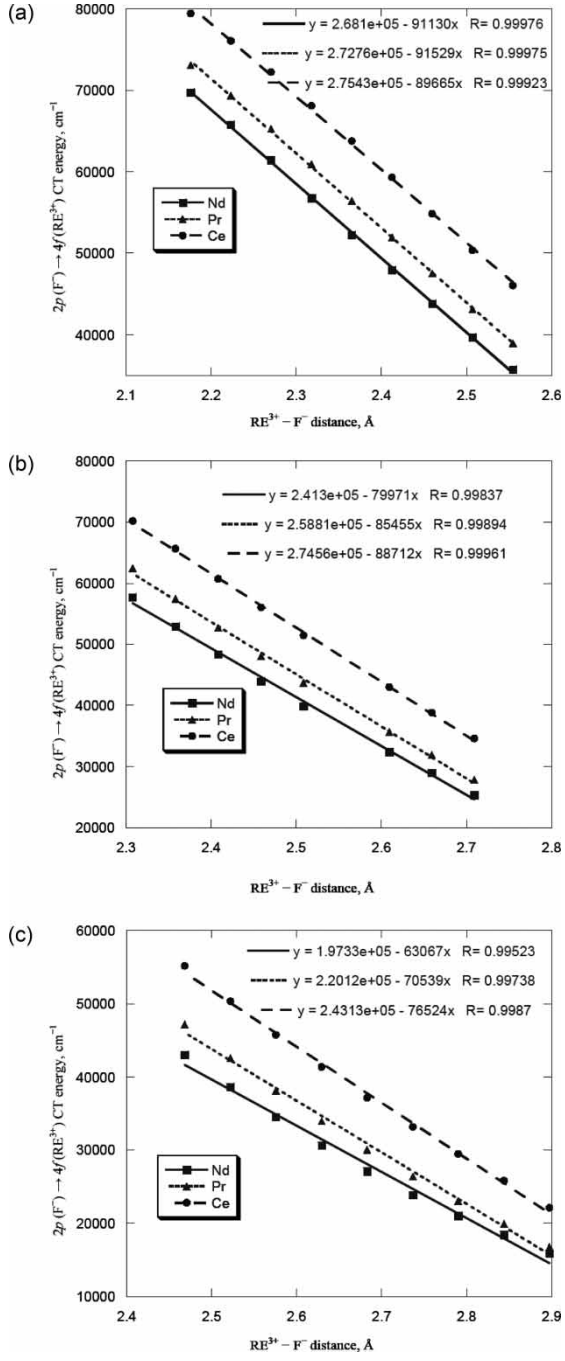

Figure 3. Dependence of $2p\ (F^-) \rightarrow 4f\ (RE^{3+})$ CT energies on RE^{3+}–F^- distance for Ce^{3+}, Pr^{3+}, Nd^{3+} in CaF_2, SrF_2, BaF_2 crystals (a, b, and c, respectively).

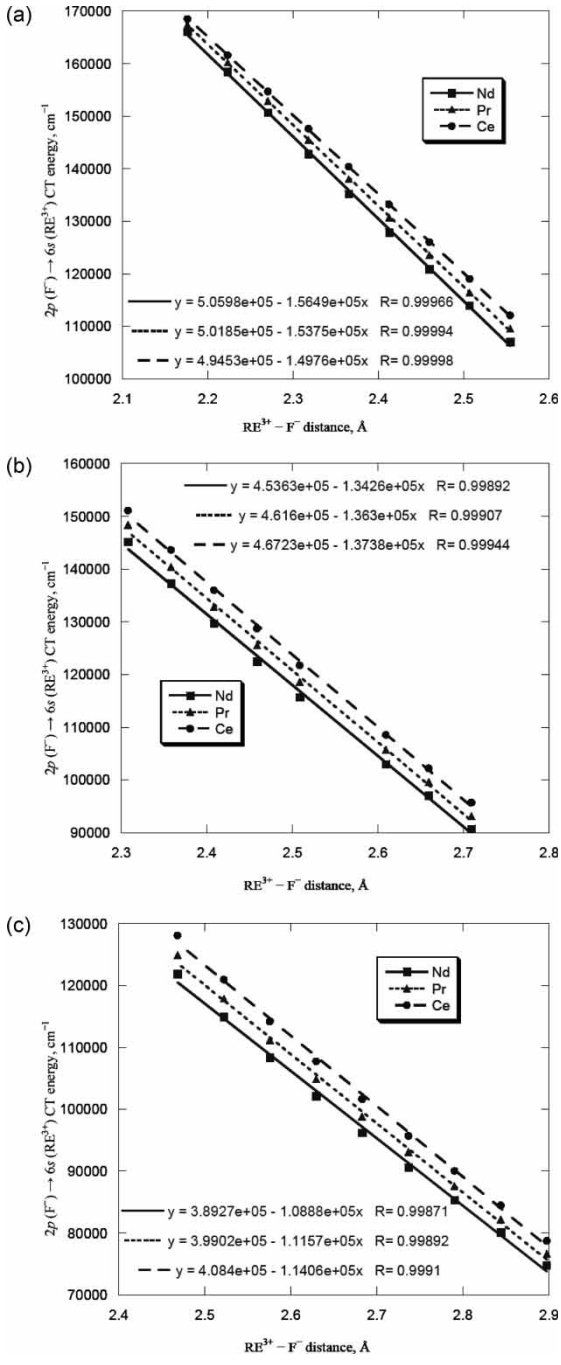

Figure 4. Dependence of $2p\ (F^-) \rightarrow 6s\ (RE^{3+})$ CT energies on RE^{3+}–F^- distance for Ce^{3+}, Pr^{3+}, Nd^{3+} in CaF_2, SrF_2, BaF_2 crystals (a, b and c, respectively).

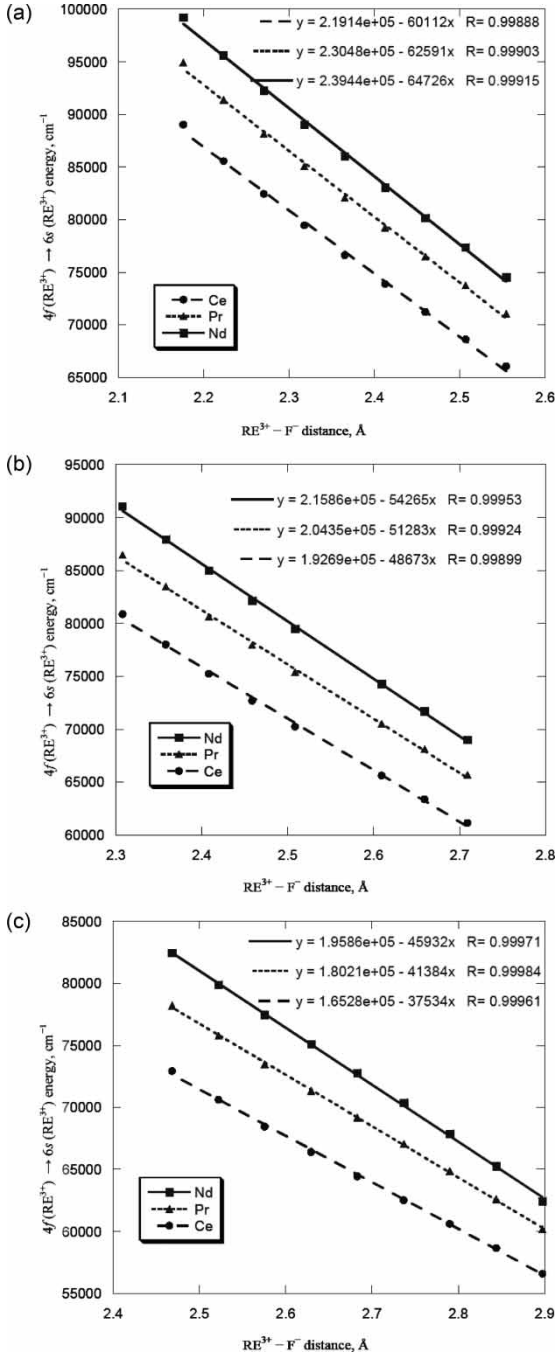

Figure 5. Dependence of $4f\,(RE^{3+}) \rightarrow 6s\,(RE^{3+})$ energies on RE^{3+}–F^{-} distance for Ce^{3+}, Pr^{3+}, Nd^{3+} in CaF_2, SrF_2, BaF_2 crystals (a, b, and c, respectively).

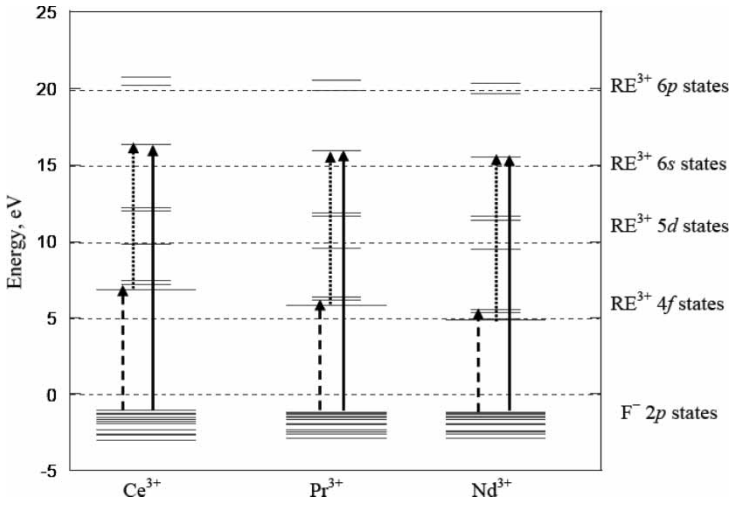

Figure 6. Relative positions of the highest MO of Ce^{3+}, Pr^{3+}, and Nd^{3+} in CaF_2. Occupied and unoccupied MO are shown by long and short horizontal lines, respectively. $2p$ (F^-) $\rightarrow$ $4f$ (RE^{3+}), $4f$ (RE^{3+})$-6s$ (RE^{3+}), and $2p$ (F^-) $\rightarrow$ $6s$ (RE^{3+}) transitions are shown by dashed, dotted, and solid arrows, respectively. Similar diagrams for SrF_2 and BaF_2 are not shown.

and Ionova et al.,[32] apart from energies of the $2p$ (F^-) $\rightarrow$ $6s$ (RE^{3+}) CT transition, which in our calculations is much higher. As follows from Figure 6, the following relation approximately holds true: E ($2p-6s$) $\approx$ E ($2p-4f$) + E ($4f-6s$) (the final state for the $2p$ (F^-) $\rightarrow$ $4f$ (RE^{3+}) transition is the lowest unoccupied $4f$ orbital, whereas the initial state for the $4f$ (RE^{3+})$-6s$ (RE^{3+}) transition is the highest occupied $4f$ orbital).

This condition is practically fulfilled for the calculated values (Table 2). No experimental data on the $2p$ (F^-) $\rightarrow$ $4f$ (RE^{3+}) CT transitions were reported in Refs. 29 and 30, but these transitions are hardly to be expected around 4000–20,000 cm^{-1} (these values would be required to make the above condition valid for the experimental values: Table 3). At least, experimental results reported by Ionova et al.[32] and Park and Oh[33] for similar transitions in rare-earth trihalides are from 53,000 cm^{-1} to 86,300 cm^{-1}. Therefore, estimation of the $2p$ (F^-) $\rightarrow$ $6s$ (RE^{3+}) CT transitions at about 80,000 cm^{-1}[29,30] can be questioned. It seems to be significantly underestimated, and spectral features around 80,000 cm^{-1} may be ascribed to the high energy tail of the $4f$ (RE^{3+})$-6s$ (RE^{3+}) transition. However, this issue needs additional experimental investigation.

A look at the coefficients of the linear approximations collected in Table 2 reveals that on average, the absolute values of the derivatives dE/dR are the largest for all ions in CaF_2, intermediate in SrF_2, and the smallest in BaF_2. This trend shows that the energies of all transitions considered in the

Table 2. Dependencies of $10Dq$ and energies of the $2p$ ($F^{—}$) $\rightarrow$ $4f$ (RE^{3+}), $4f$ (RE^{3+})–$6s$ (RE^{3+}), $2p$ ($F^{—}$) $\rightarrow$ $6s$ (RE^{3+}) transitions on the RE^{3+}–$F^{—}$ distance R in CaF_2, SrF_2, BaF_2 crystals[a]

	$10Dq$	$2p$ ($F^{—}$) $\rightarrow$ $4f$ (RE^{3+})	$4f$ (RE^{3+})–$6s$ (RE^{3+})	$2p$ ($F^{—}$) $\rightarrow$ $6s$ (RE^{3+})
CaF_2				
Ce^{3+}	$\frac{1.7060 \times 10^6}{R^{5.2884}}$	$2.7643 \times 10^5 - 89{,}665\ R$	$2.1914 \times 10^5 - 60{,}112\ R$	$4.9453 \times 10^5 - 1.4976 \times 10^5\ R$
Pr^{3+}	$\frac{1.6187 \times 10^6}{R^{5.2684}}$	$2.7276 \times 10^5 - 91{,}529\ R$	$2.3048 \times 10^5 - 62{,}591\ R$	$5.0185 \times 10^5 - 1.5375 \times 10^5\ R$
Nd^{3+}	$\frac{1.5373 \times 10^6}{R^{5.2461}}$	$2.6810 \times 10^5 - 91{,}130\ R$	$2.3944 \times 10^5 - 64{,}726\ R$	$5.0598 \times 10^5 - 1.5649 \times 10^5\ R$
SrF_2				
Ce^{3+}	$\frac{1.6320 \times 10^6}{R^{5.2539}}$	$2.7456 \times 10^5 - 88{,}712$ R	$1.9269 \times 10^5 - 48{,}673\ R$	$4.6723 \times 10^5 - 1.3738 \times 10^5\ R$
Pr^{3+}	$\frac{1.5050 \times 10^6}{R^{5.2049}}$	$2.5881 \times 10^5 - 85{,}455\ R$	$2.0435 \times 10^5 - 51{,}283\ R$	$4.6160 \times 10^5 - 1.3630 \times 10^5\ R$
Nd^{3+}	$\frac{1.4118 \times 10^6}{R^{5.1690}}$	$2.4130 \times 10^5 - 79{,}971$ R	$2.1586 \times 10^5 - 54{,}265\ R$	$4.5363 \times 10^5 - 1.3426 \times 10^5\ R$
BaF_2				
Ce^{3+}	$\frac{1.3465 \times 10^6}{R^{5.0802}}$	$2.4313 \times 10^5 - 76{,}524\ R$	$1.6528 \times 10^5 - 37{,}534\ R$	$4.0840 \times 10^5 - 1.1406 \times 10^5\ R$
Pr^{3+}	$\frac{1.2863 \times 10^6}{R^{5.0642}}$	$2.2012 \times 10^5 - 70{,}539\ R$	$1.8021 \times 10^5 - 41{,}384\ R$	$3.9902 \times 10^5 - 1.1157 \times 10^5\ R$
Nd^{3+}	$\frac{1.2387 \times 10^6}{R^{5.0558}}$	$1.9733 \times 10^5 - 63{,}067\ R$	$1.9586 \times 10^5 - 45{,}932\ R$	$3.8927 \times 10^5 - 1.0888 \times 10^5\ R$

[a]In all equations, R is measured in Å, and the result is the energy measured in $cm^{—1}$.

Table 3. Energies (in 1000 cm^{-1}) of some CT and intraconfigurational transitions for Ce^{3+} and Pr^{3+} in CaF_2, SrF_2, BaF_2 crystals

	$2p$ (F^-) → $4f$ (RE^{3+})		$4f$ (RE^{3+})–$6s$ (RE^{3+})		$2p$ (F^-) → $6s$ (RE^{3+})		$4f$ (RE^{3+}) → $5d$ (RE^{3+})[a]	
	Exp.	Calc.	Exp.	Calc.	Exp.	Calc.	Exp.	Calc.
				CaF_2				
Ce^{3+}	—	≈47.2	≈60–77[29]	≈66.1	≈80[29]	≈113.3	≈31–56[29]	≈21–51
Pr^{3+}	—	≈43.7	≈76[30]	≈73.9	≈80[30]	≈117.2	≈44–69[30]	≈31–57
				SrF_2				
Ce^{3+}	—	≈45.5	≈60–77[29]	≈67.0	≈80[29]	≈112.7	≈31–56[29]	≈23–45
Pr^{3+}	—	≈41.6	≈76[30]	≈74.0	≈80[30]	≈115.0	≈44–69[30]	≈30–51
				BaF_2				
Ce^{3+}	—	≈45.3	≈60–77[29]	≈73.0	≈80[29]	≈113.5	≈31–56[29]	≈26–40
Pr^{3+}	—	≈37.5	≈76[30]	≈68.3	≈80[30]	≈110.2	≈44–69[30]	≈30–47

[a]Multiplet structure was not considered when estimating the $4f$ (RE^{3+}) → $5d$ (RE^{3+}) transition energies, that is why the lowest values are a little underestimated.

current paper are more sensible to the variation of interionic separations in CaF_2, and then this sensibility decreases when going to crystals with larger lattice parameter.

CONCLUSIONS

As a result of systematic *ab initio* microscopic analysis, the functional dependencies of $10Dq$ and energies of several types of CT and interconfigurational transitions on the chemical bond length were obtained for the $[REF_8]^{5-}$ (RE = Ce, Pr, Nd) units in CaF_2, SrF_2, and BaF_2 crystals. No empirical or fitting parameters were used in the calculations. Because all calculations are entirely based on the MO concept, not only Coulomb interaction (which itself is not sufficient to reproduce the experimental results properly) but also covalent effects and configuration interaction have been taken into account. A simple point charge approximation describes dependence of $10Dq$ on distance as $1/R^5$, whereas the more elaborated approach in the current study shows $n > 5$ for all considered systems. Calculated values of $10Dq$ decrease with increasing RE^{3+} atomic number in each considered crystal. Increase of the crystal lattice constant in the series $CaF_2 < SrF_2 < BaF_2$ is accompanied by decrease of $10Dq$. For all crystals, the values of n follow the trend: $n(Ce^{3+}) > n(Pr^{3+}) > n(Nd^{3+})$.

Dependence of the energies of considered CT and interconfigurational transitions on R is linear for all considered crystals; all these energies decrease when R increases. Functional dependencies found in the current work can be used for analysis of the pressure dependence of absorption spectra of fluoride crystals doped with light lanthanides. Estimated energies of the $2p\ (F^-) \rightarrow 4f\ (RE^{3+})$ and $4f\ (RE^{3+})$–$6s\ (RE^{3+})$ agree with experimental data. Comparison of the calculated and previously reported[29,30] energies of the $2p\ (F^-) \rightarrow 6s\ (RE^{3+})$ CT transitions together with analysis of the relative positions of the calculated MO suggests that the values reported by Loh were underestimated by about 20,000–35,000 cm^{-1}.

In general, the DVME method is a reliable tool for the microscopic analysis of the spectroscopic parameters of RE ions in crystals. Computational technique can be applied in a straightforward way to other systems with di- and trivalent lanthanides.

ACKNOWLEDGMENTS

This work was partially supported by the following programs: the "Open Research Center" Project for Private Universities, matching fund subsidy from MEXT (Japanese Ministry of Education, Culture, Sports, Science and Technology), 2004–2008; and by the Computational Materials Science Unit

at Kyoto University. K.O. was supported by the individual special research subsidy from Kwansei Gakuin University.

REFERENCES

1. Dieke, G. H. *Spectra and Energy Levels of Rare Earth Ions in Crystals*; Wiley Interscience: New York, 1968.
2. Görller-Walrand, C.; Binnemans, K. *Handbook on the Physics and Chemistry of Rare Earths*; Gschneidner, J. K. A. and Eyring, L., (eds.); North-Holland: Amsterdam, 1996 Vol. 23, pp. 121–283.
3. Meijerink, A.; Wegh, R. T. VUV spectroscopy of lanthanides: extending the horizon. *Mater. Sci. Forum* **1999**, *315–317*, 11–26.
4. Wegh, R. T.; Meijerink, A. Spin-allowed and spin-forbidden $4f^n \leftrightarrow 4f^{n-1}5d$ transitions for heavy lanthanides in fluoride hosts. *Phys. Rev. B* **1999**, *60*, 10820–10830.
5. Wegh, R. T.; Meijerink, A.; Lamminmäki, R. J. Hölsä, J. Extending Dieke's diagram. *J. Lumin.* **2000**, *87–89*, 1002–1004.
6. Dorenbos, P. The 5d level positions of the trivalent lanthanides in inorganic compounds. *J. Lumin.* **2000**, *91*, 155–176.
7. Dorenbos, P. The $4f^n \leftrightarrow 4f^{n-1}5d$ transitions of the trivalent lanthanides in halogenides and chalcogenides. *J. Lumin.* **2000**, *91*, 91–106.
8. Reid, M. F.; van Pieterson, L.; Wegh, R. T.; Meijerink, A. Spectroscopy and calculations for $4f^N \rightarrow 4f^{N-1}5d$ transitions of lanthanide ions in $LiYF_4$. *Phys. Rev. B* **2000**, *62*, 14744–14749.
9. van Pieterson, L.; Reid, M. F.; Burdick, G. W.; Meijerink, A. $4f^n \leftrightarrow 4f^{n-1}5d$ transitions of the light lanthanides: experiment and theory. *Phys. Rev. B* **2002**, *65*, 045113.
10. van Pieterson, L.; Reid, M. F.; Burdick, G. W.; Meijerink, A. $4f^n \leftrightarrow 4f^{n-1}5d$ transitions of the heavy lanthanides: experiment and theory. *Phys. Rev. B* **2002**, *65*, 045114.
11. Dorenbos, P. Systematic behavior in trivalent lanthanide charge transfer energies. *J. Phys. Condens. Matter* **2003**, *15*, 8417–8434.
12. Tanner, P. A.; Mak, C. S. K.; Faucher, M. D.; Kwok, W. M.; Philips, D. L.; Mikhailik, V. $4f–5d$ Transitions of Pr^{3+} in elpasolite lattices. *Phys. Rev. B* **2003**, *67*, 115102.
13. Ning, L. X.; Duan, C. K.; Xia, S. D.; Reid, M. F.; Tanner, P. A. A model analysis of $4f^n–4f^{n-1}5d$ transitions of rare-earth ions in crystals. *J. Alloys Compd.* **2004**, *366*, 34–40.
14. Tanner, P. A. Spectra, energy levels and energy transfer in high symmetry lanthanide compounds. *Topics Curr. Chem.* **2004**, *241*, 167–278.
15. Ogasawara, K.; Watanabe, S.; Toyoshima, H.; Ishii, T.; Brik, M. G.; Ikeno, H.; Tanaka, I. Optical spectra of trivalent lanthanides in $LiYF_4$ crystal. *J. Solid State Chem.* **2004**, *178*, 412–418.
16. Shi, J. S.; Wu, Z. J.; Zhou, S. H.; Zhang, S. Y. Dependence of crystal field splitting of 5d levels on hosts in halide crystals. *Chem. Phys. Lett.* **2003**, *380*, 245–250.
17. Ogasawara, K.; Iwata, T.; Koyama, Y.; Ishii, T.; Tanaka, I.; Adachi, H. Relativistic cluster calculation of ligand-field multiplet effects on cation L_2, L_3 X-ray absorption edges of $SrTiO_3$, NiO, and CaF_2. *Phys. Rev. B* **2001**, *64*, 115413.

18. Rosén, A.; Ellis, D. E.; Adachi, H.; Averill, F. W. Calculations of molecular ionization energies using a self-consistent charge Hartree-Fock-Slater method. *J. Chem. Phys.* **1976**, *65*, 3629–3634.
19. Ogasawara, K.; Watanabe, S.; Sakai, Y.; Toyoshima, H.; Ishii, T.; Brik, M. G.; Tanaka, I. Calculations of complete $4f^n$ and $4f^{n-1}5d^1$ energy level schemes of free trivalent rare-earth ions. *Jpn. J. Appl. Phys.* **2004**, *43*, L611–L613.
20. Ogasawara, K.; Watanabe, S.; Ishii, T.; Brik, M. G. Relativistic calculations of complete $4f^n$ energy level schemes of free trivalent lanthanides. *Jpn. J. Appl. Phys.* **2005**, *44*, 7488–7490.
21. Ikeno, H.; Tanaka, I.; Koyama, Y.; Mizoguchi, T.; Ogasawara, K. First-principles multielectron calculations of Ni $L_{2,3}$ NEXAFS and ELNES for $LiNiO_2$ and related compounds. *Phys. Rev. B* **2005**, *72*, 075123.
22. Brik, M. G. Comparative first-principles analysis of the absorption spectra of $ZnAl_2S_4$ and $ZnGa_2O_4$ crystals doped with Cr^{3+}. *Eur. Phys. J. B* **2006**, *49*, 269–274.
23. Brik, M. G. Fully relativistic analysis of the covalence effects for the isoelectronic $3d^3$ ions (Cr^{3+}, Mn^{4+}, Fe^{5+}) in $SrTiO_3$. *J. Phys. Chem. Solids* **2006**, *67*, 856–861.
24. Zhurova, E. A.; Maximov, B. A.; Simonov, V. I.; Sobolev, B. P. Structural studies of CaF_2 (at 296 K) and Ca_{1-x} Pr_x F_{2+x}, $x = 0.1$ (at 296 and 170 K) crystals. *Kristallografiya* **1996**, *41*, 438–443.
25. Forsyth, J. B.; Wilson, C. C.; Sabine, T. M. Time-of-flight neutron diffraction study of anharmonic thermal vibrations in SrF_2, at the spallation neutron source ISIS. *Acta Cryst. A* **1989**, *45*, 244–247.
26. Radtke, A. S.; Brown, G. E. Frankdicksonite, BaF_2, a new mineral from Nevada. *American Mineralogist* **1974**, *59*, 885–888.
27. Sugano, S.; Tanabe, Y.; Kamimura, H. *Multiplets of Transition-Metal Ions in Crystals*; Academic Press: New York, 1970.
28. Moreno, M.; Barriuso, M. T.; Aramburu, J. A.; García-Fernández, P.; García-Lastra, J. M. Microscopic insight into properties and electronic instabilities of impurities in cubic and lower symmetry insulators: the influence of pressure. *J. Phys. Condens. Matter* **2006**, *18*, R315–R360.
29. Loh, E. Ultraviolet absorption spectra of Ce^{3+} ion in alkaline-earth fluorides. *Phys. Rev.* **1967**, *154*, 270–276.
30. Loh, E. Ultraviolet absorption spectra of Pr^{3+} ion in alkaline-earth fluorides. *Phys. Rev.* **1967**, *158*, 273–279.
31. Wissing, K.; Aramburu, J. A.; Barriuso, M. T.; Moreno, M. Optical properties due to Cr^{4+} in oxides: density functional study. *Solid State Commun.* **1998**, *108*, 1001–1005.
32. Ionova, G.; Krupa, J. C.; Gérard, I.; Guillaumont, R. Systematic in electron-transfer energies for lanthanides and actinides. *New J. Chem.* **1995**, *19*, 677–689.
33. Park, K.-H.; Oh, S.-J. Electron-spectroscopy study of rare-earth trihalides. *Phys. Rev. B* **1993**, *48*, 14833–14842.